Proliferation and osteogenic differentiation of mesenchymal stem cells on three-dimensional scaffolds made by thermal sintering method

FARID MALEKI [1], HAFEZ JAFARI[2], PEJMAN GHAFFARI[3], MOHSEN SHAHROUSVAND [4], GITY MIR MOHAMAD SADEGHI[*1], HOUMAN ALIMORADI[5], , AMIN SHAVANDI [2*]

[1] *Department of Polymer Engineering and Color Technology, Amirkabir University of Technology, Tehran, Iran.*

[2]*BioMatter-Biomass Transformation Lab (BTL), École polytechnique de Bruxelles, Université libre de Bruxelles (ULB), Avenue F.D. Roosevelt, 50 – CP 165/61, 1050 Brussels, Belgium*

[3]*Nano-Biopolymers Research Laboratory, School of Chemical Engineering, College of Engineering, University of Tehran, PO Box: 11155-4563, Tehran, Iran*

[4]*Caspian Faculty of Engineering, College of Engineering, University of Tehran, PO Box 119-43841, Chooka Branch, Rezvanshahr, 4386156387, Guilan Province, Iran*

[5]*School of Biomedical Sciences, University of Otago, Dunedin, New Zealand*

[*]Corresponding author, e-mail: gsadeghi@aut.ac.ir, amin.shavandi@ulb.be

Received [Dates will be filled in by the Editorial office]

Abstract

This article presents a thermal sintering method to fabricate porous bone tissue engineering scaffolds based on polycaprolactone (PCL), polylactic acid (PLA), and their composites. The mechanical properties, porous structure, biodegradability, and biocompatibility of sintered scaffolds were evaluated. The scaffolds showed a porosity in the range of 86-91% with a pore size of 75 μm to 400 μm. PCL/PLA composite scaffolds showed a' Young's modulus of around 49 MPa, which was between the modulus values of PCL (24 MPa) and PLA (63 MPa) scaffolds. Fibroblast cells (SNL) exhibited spreading, and adhesion on the scaffolds, and Scaffolds demonstrated a significant difference in the osteogenic differentiation of human Mesenchymal Stem Cells (hMSCs) after 7 and 14 days of culture in comparison to the control (tissue culture polystyrene). Our results demonstrated that the thermal sintered PCL/PLA composite scaffold could be a promising candidate for bone tissue regeneration.

Keywords: Bone tissue engineering; Scaffold fabrication; Thermal sintering method; human Mesenchymal Stem Cells (hMSCs).

Introduction

In tissue engineering and in-situ tissue reconstruction, porous 3D scaffolds prepared by biodegradable polymers are widely used as temporary extracellular matrices(Koons, Diba et al. 2020). An ideal scaffold for cell/tissue engineering must mimic the anatomical and physiological conditions of the target tissue. Hence, the designed scaffolds must possess proper mechanical properties and allow sufficient transport of nutrients and waste to match the degradation or resorption rate required for tissue development (Shavandi, Bekhit et al. 2015, Qu, Fu et al. 2019). To this end, biocompatibility, biodegradability, high porosity with a uniform pore distribution and interconnectivity, and large specific surface area are essential characteristics of tissue engineering scaffolds (Shavandi, Bekhit et al. 2016).

The use of biodegradable polymers, with numerous biomedical applications, has been increased during the past decades. Among a wide range of synthetic polymers, polylactic acid (PLA) and poly (ε-caprolactone) PCL have been approved by FDA biomedical applications (Park, Lee et al. 2017). Thanks to their unique properties, such as biocompatibility,

biodegradability, and relatively high mechanical properties, PLA and PCL have been frequently used for tissue engineering (Yao, Cosme et al. 2017, Shahrezaee, Salehi et al. 2018). PCL hydrophobicity and higher crystallinity compared to the PLA lead to a slower degradation rate for PCL (Yao, Cosme et al. 2017). In contrast, PLA has higher stiffness and different degradation kinetic compared to the PCL. PLA degradation mechanism includes chain scission and subsequently fragmentation, while PCL degradation is due to the scission of the end groups of the polymer chains (Barral, Dropsit et al. 2021).

Compositing PLA and PCL (PCL/PLA blend) has been widely investigated to fabricate biomaterials composites due to the maintenance of both polymers' merits and improving PLA mechanical properties, crystallization rate, and degradation rate (Sun and Downes 2009, Vieira, Vieira et al. 2011). Several techniques such as solvent casting, leaching methods, and gas foaming have been carried out to develop three-dimensional (3D) PCL-based scaffolds (Jafari, Shahrousvand et al. 2018, Jafari, Shahrousvand et al. 2020, Nahanmoghadam, Asemani et al. 2021). However, poor mechanical stability and large scale-up limitations hindered applying these methods to design porous scaffolds (Luciani, Coccoli et al. 2008).

The thermal sintering of polymers is a promising approach for constructing porous, interconnected 3D scaffolds (Shin, Abukawa et al. 2008, Nail, Zhang et al. 2015, Naghieh, Ravari et al. 2016). Luciani et al. reported ease of tunability in mechanical properties, porosity, and interconnectivity of thermally sintered PCL scaffolds (Luciani, Coccoli et al. 2008). PCL/PLA composite scaffold developed by the melt-blending method showed 100 % interconnectivity and porous structure. The addition of PLA to the PCL (1:1) also enhanced the biomechanical performance of the scaffolds (Patrício, Domingos et al. 2014). Moreover, a series of PCL/PLA foam blends via the foaming process demonstrated an open-cell structure with high interconnectivity resulted in the viability and migration HUVECs cells (Lv, Zhao et al. 2018).

This research aimed to prepare scaffolds using PLA, PCL, and PCL/PLA (1:1 wt. %) by the thermal sintering method. The scaffolds' physiochemical and biological properties such as morphology, porosity, water uptake, biodegradability, mechanical properties, cell attachment, and cell viability were investigated. Moreover, the osteogenic differentiation capacity of sintered scaffolds was determined via alkaline phosphate (ALP) and calcium content. We hypothesize that the PCL/PLA composite scaffold with porous structure can facilitate cell proliferation, attachment as well as osteogenic differentiation of human Mesenchymal Stem Cells (hMSCs).

Experimental

Materials

The PLA used in this study was from Nature Works LLC (Minnetonka, MN) (PLA 2002D,containing 1.5–2.0% of D isomer, M_n= 127,000, D=1.25 g/cm^3, and T_g=52-56 ˚C) . Poly (e-caprolactone) (PCL) was purchased from Sigma Aldrich (440744, St. Louis, MO, USA) with a Mn of 80,000 g/mol and a Tm of 58–60 ˚C.

Fabrication of the scaffolds

PLA pellets were initially dried using a vacuum oven at 80 °C overnight (VD 53, Binder, Tuttlingen, Germany) to reduce moisture. Then, the PLA and PCL pellets were ground in liquid nitrogen using a small mixer (Mathieu, Bourban et al. 2006) and passed through a sieve (500 µm pore size, mesh No. 35) to remove the aggregates. Then, PLA, PCL, and the composite mixture (1:1) powder were poured into an in-house-built metal mold with a length and width of 44 and 23 mm and was heated in an oven at 160 °C (Heating oven ED 23, Binder, Tuttlingen, Germany) (Patrício, Domingos et al. 2014, Rao, Venkatanarayana et al. 2019) for 60 min. It then was quickly transformed into a container of water and ice for 20 seconds until it reaches room temperature. The scaffolds were removed from the mold and kept in a desiccator for further investigation.

Physicochemical properties analysis

The changes in the chemical structure or composition of the polymers were followed by FTIR (Thermo Nicolet Nexus 870 with 100 scans) over the range of 400–4000 cm^{-1} with 2 cm^{-1} spectral resolution. Morphology of PLA, PCL and PLA/PCL composites scaffolds (1:1 wt. %) and cell attachment was studied using a scanning electron microscope (SEM, Stereocan S 360-Leica Cambridge, made in England). 5 images with different magnification (×500 and ×1000) from each sample were taken. The 50 pores/scaffold size was measured using KLONK Image Measurement Light software (Edition 11.2.0.0) (Ghorbani, Zamanian et al. 2019).

The scaffolds' porosity was calculated using a specific gravity bottle according to Archimedes' Principle (Yang, Shi et al. 2002, Shahrousvand, Tabar et al. 2017) by placing the scaffolds (5 replicates per scaffold) into ethanol of 96 % for 45 min within a desiccator connected a vacuum pump (V-600, Buchi Italia srl, Cornaredo, Italy) using formula (1).

$$Porosity\ volume\ of\ \ the\ scaffolds\ = (W_w - W_0)/\rho \qquad (1)$$

$$\text{Porosity percentage} = \text{porosity volume / total volume} \qquad (2)$$

Where W_w, W_0 and ρ (ρ_{PLA}= 1.25, ρ_{PCL}= 1.145, $\rho_{PLA/PCL}$= 1.19 g/mL at 25 ˚C) are wet scaffold weight, dried sample weight and density of scaffolds, respectively

Tensile strength and Young's modulus were determined using a mechanical tensile tester (Instron 1122) at room temperature and relative humidity of 50 ± 2 % (Sun and Downes 2009, Jafari, Shahrousvand et al. 2020). A crosshead speed of 5 mm/min was used, and the cross area was (3.8 × 0.06) mm^2. The grip distance was 35 mm, and the full-scale load was set at 0.005 kN.

Water uptake

Water uptake of the scaffolds was measured by immersing the scaffolds in distilled water for 6 days (Meskinfam, Bertoldi et al. 2018), and then at determined time intervals, the scaffolds were taken out and dried by removing the free water on the surface with a filter paper and weighed (W1). Then the scaffolds were thoroughly vacuum-dried at 70 °C for 24 h and weighed again (W2). The water uptake could be calculated as follows, and three specimens were averaged.

$$\text{water uptake}(\%) = \frac{(W_1 - W_2)}{W_2} \times 100 \qquad (2)$$

Accelerated degradation and biodegradation

The accelerated degradation rate of scaffolds was investigated according to our previous article (Jafari, Shahrousvand et al. 2018). The scaffolds were immersed into 15 ml of NaOH (1 M) and placed in an oven at 60 °C for 24 h. After 2, 6, 18 and 24 h the scaffolds were removed, washed with distilled water and dried using a vacuum oven at 70 °C for 24 h. The remaining mass was calculated according to Eq. (3).

$$\text{Remaining Mass } (\%) = 100 - \left(\frac{(M_i - M_f) \times 100}{M_i}\right) \qquad (3)$$

Where M_i is the initial sample mass, and M_f is the mass after degradation.

The biodegradation of the scaffolds was carried out in an incubator at 37 °C in the simulated body fluid (SBF) solution (Jafari, Shahrousvand et al. 2018). Briefly, the scaffolds were weighed accurately and immersed in 20 mL of the SBF solution, and the degradation was

monitored over 90 days. The samples were removed at predetermined time intervals, washed with distilled water, and dried in a vacuum oven at 70 °C for 24 h. The degradation rate of samples was evaluated via measuring the scaffold's remaining mass according to Eq. (3). All experiments were performed in three replicates.

Cytotoxicity and cell attachment on scaffolds

The fibroblast cells (SNL76/7) and Mesenchymal Stem Cells (hMSCs) were obtained from the Stem Cell Technology Research Center (Tehran, Iran). The cells were cultured in Dulbecco's modified eagle medium (DMEM) supplemented with 10 % fetal bovine serum (FBS), penicillin G sodium (10 units·ml^{-1}), and streptomycin sulphate (10 mg·ml^{-1}) (Gibco BRL, NY, USA) in a humidified atmosphere of 5 % CO_2 at 37 °C (Jafari, Delporte et al. 2021). Culture media was replaced every 48 h until reaching 80 % cell confluency, and the cells at passage 5 were used for the study. The cytotoxicity of scaffolds was analyzed by MTT (3-(4,5-dimethylthiazol-2-yl)-2,5-diphenyltetrazolium bromide) tetrazolium reduction assay (Ghaffari-Bohlouli, Jafari et al. 2021). After sterilizing the scaffolds using ethanol (70 % w/w) and UV radiation, the scaffolds were washed with PBS 3 times prior to the experiment. The SNL76/7 cells were seeded on top of the scaffolds at a density of 10,000 cells/well into a 48-well plate and incubated at 37 °C for 7 days. The cell viability was investigated MTT assay. At 1, 4 or 7 days after the seeding, MTT solution was added to the wells and the cells were incubated for 3h in a humidified atmosphere of 5 % CO_2 at 37 °C. Then, the MTT solution was removed and replaced with DMSO to dissolve the formazan crystals. The optical density (OD) of wells was measured using an ELISA plate reader at 570 nm, and cell viability of the samples was evaluated via comparing the OD of samples to the control (Tissue Culture Polystyrene (TCPS)).

For the cell attachment study, after seeding the cells in a 48-well plate (as described above), the scaffolds were fixed and dehydrated with 30, 50, 75, 95 and 100% gradients of ethanol following the previously described protocol (Shahbazarab, Teimouri et al. 2018). Several SEM images were taken from each scaffold at the scales of 50 and 200 µm. To analyze the images, ImageJ (open-source imaging software) was used. The specimens were coated with gold prior to the SEM observations. All experiments were carried out in three replicates.

Osteogenic differentiation

For osteogenic induction of hMSCs, the basal medium was replaced with an osteogenic medium as described earlier (Shahrousvand, Tabar et al. 2017), which contained DMEM supplemented with 10 % FBS, 50 mg.mL^{-1} ascorbic acid 2-phosphate, 10 nM dexamethasone and 10 mM β-glycerophosphate . The cultures were then placed in an incubator at 37 °C with 5% CO_2 for two weeks.

Alkaline phosphatase (ALP) activity

Osteogenic differentiation of hMSCs was measured using ALP as a marker of osteogenesis according to the protocol described (Shamsi, Karimi et al. 2017). The plates were washed three times with ice-cold PBS on days 7 and 14. Radio-immune precipitation (RIPA) lysis buffer was used to extract the total protein of the cells on Tissue Culture Polystyrene (TCPS) and scaffolds. An ALP assay kit (Parsazmun, Tehran, Iran) was used to measure ALP activity in the lysate after centrifugation at 15,000 g for 15 min at 4 ºC to sediment cell debris. P-nitrophenyl phosphate was used as the substrate for the determination of alkaline phosphatase activity levels. The activity of the enzyme (IU/l) was normalized against the total protein (mg). The fluorescence intensity was determined at 480 nm excitation and 520 nm emission using a microplate reader (BioTek Instruments, USA).

Calcium content analysis

After 7 and 14 days of hMSCs culture, the calcium mineral contents deposited on the scaffolds and TCPS induced by hMSCs were determined by a calcium assay kit (Parsazmun, Tehran, Iran) according to the method described (Shahrousvand, Tabar et al. 2017). The samples were homogenized in 0.6 M hydrochloric acid and were shaken for 4 h at 4 °C for performing the calcium extraction. The kit reagent was added to the samples and transferred into vials. Then, the OD of scaffolds and control (TCPS) was measured at 570 nm. Calcium content was determined using a standard concentration curve of serial dilutions of calcium versus corresponding OD.

Statistical analysis

Values were expressed as mean ± SD. Levels of significance were calculated using a two-way analysis of variance (ANOVA) followed by Bonferroni's post hoc test. Differences were considered statistically significant at $P \leq 0.05$.

Results and discussion

FTIR spectra peaks analysis

The PLA, PCL, and PLA/PCL composite scaffolds were analyzed by FTIR to inspect the functional groups and determine the potential chemical interactions between them. Figure 1 (a) shows the FTIR spectra of the functional groups of the PLA, PCL, and PLA/PCL scaffolds. Also, the structure of the PLA and PCL are shown in figure 1 (b and c). The FTIR spectra peak of the PLA/PCL showed the same peaks that were seen in the FTIR spectra peaks of the PLA and PCL. Furthermore, no new peak was observed for the PLA/PCL at the wavenumber of 500

to 3500 cm^{-1}, which means the PLA and PCL had no chemical interaction or chemical decomposition during the process (figure 1 (a)). Fang et al.(Fang, Zhang et al. 2010) prepared nanofibers scaffolds based on the PLA, PCL, and hydroxyapatite with different ratios. Their FTIR analysis illustrated that two polymers (PLA and PCL) did not have a chemical reaction with each other. Also, they concluded that the PLA and PCL were mixed well because the density of the peak changed with alteration in the mass ratio of each component. The wavenumbers of some of the peaks in PLA and PCL were shifted to higher or lower wavenumbers at the FTIR spectra peaks of the PLA/PCL. For example, the peak with the wavenumber of 1084 and 1097 cm^{-1} attributed to −C−O symmetric stretch bond of the PLA and PCL respectively was shifted to 1076 cm^{-1} for the PLA/PCL. Other changes in the spectra of PLA/PCL compared to the PLA and PCL are listed in table 1. Potential weak physical interactions between the PLA and PCL could be attributed to the observed shifts in the FTIR spectra of the scaffolds (Lu and Kazarian 2020).

Table 1. The FTIR spectra peak assignments of functional groups for the PLA, PCL, and PLA-PCL(Fang, Zhang et al. 2010, Ghaffari-Bohlouli, Zahedi et al. 2020, Ghaffari-Bohlouli, Jafari et al. 2021).

Assignments	**PLA**	**PCL**	**PLA/PCL**
	position (cm^{-1})	position (cm^{-1})	position (cm^{-1})
−C−O symmetric stretch	1084	1097	1076
C−O−C asymmetric stretch	1180	1238	1182
−CH2	1384, 1458	1384, 1460	1379, 1455
C−H	2944, 2997	2881, 2931	2929, 2999

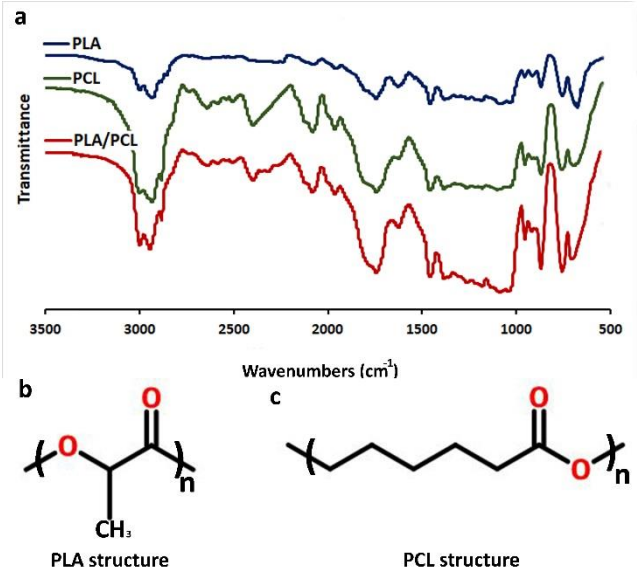

Fig. 1. (a) FTIR spectra of PLA, PCL and PLA/PCL composite scaffolds, (b) chemical structure of PCL and PLA.

All of the scaffolds had a structure with high porosity and a wide range of pores size. Figure 3 represents the percentage distribution of pores and porosity percentage of the PLA, PCL, and PLA/PCL scaffolds., The PLA scaffold had the highest porosity (90.6 %) among other samples; the PLA/PCL scaffold with a porosity of 87.3 % had more porosity compared to the PCL scaffold with a porosity of 86.6 % (figure 3 (a)). Although the PLA scaffold had the highest porosity percentage, the average size of the pores was the smallest (168±8 μm) (figure 3 (b)) among the other scaffolds.

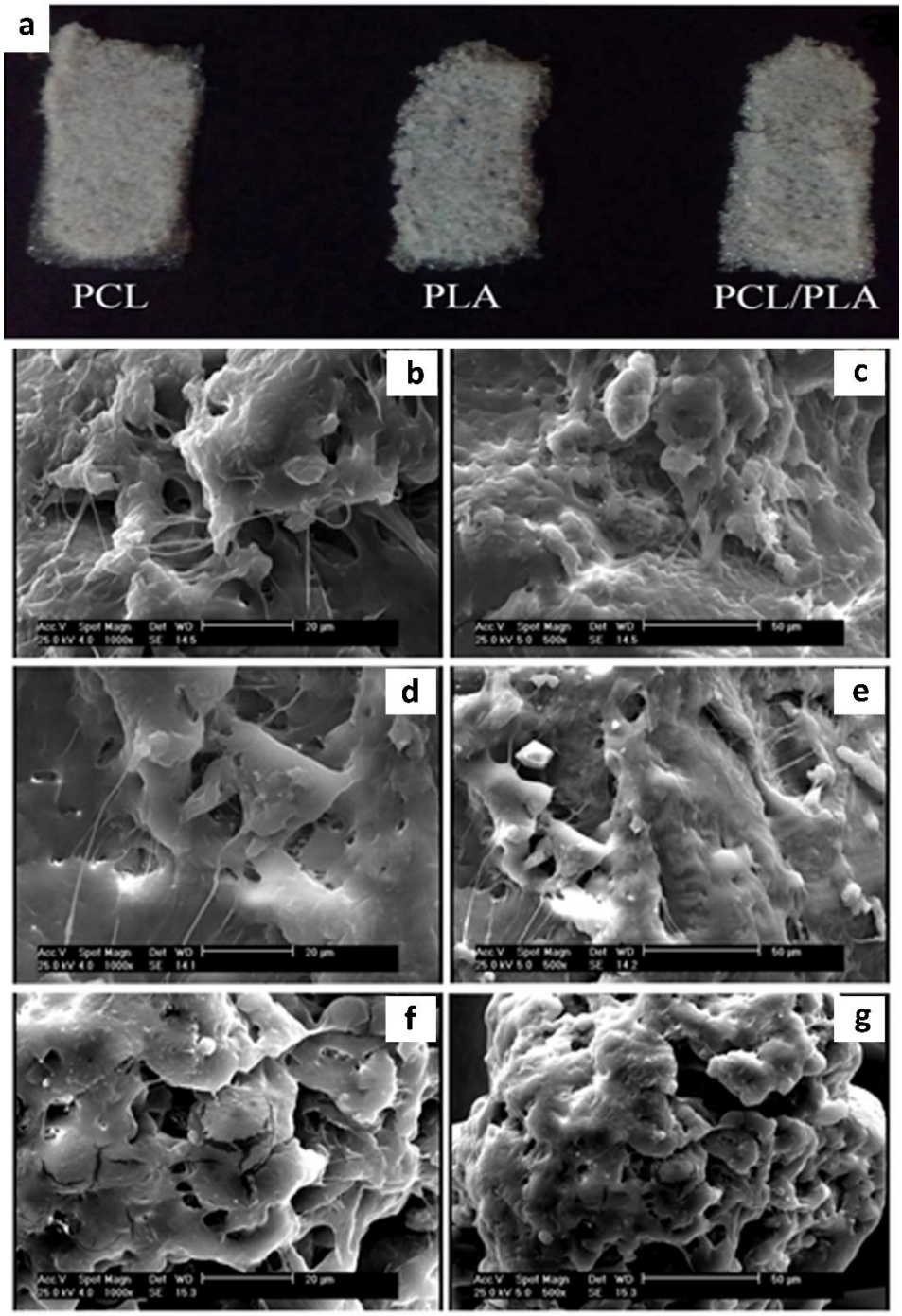

Fig. 2. (a) macrograph image of the fabricated PLA, PCL, and PLA/PCL scaffolds using the sintering method. SEM micrograph images of different scaffolds; (b and c) PLA, (d and e) PCL, and (f and g) PLA/PCL with two magnifications (500X and 1000X).

The broadest range of pores size belonged to the PLA/PCL composite scaffolds with the pore size of 75±3 μm to 400±17 μm with an average of 197±9 μm (figure 3 (d)). The difference in size between the most significant pore with the smallest pore in the PCL scaffold was 270±12 µm (figure 3 (b)). Thus, all the scaffolds had a wide range of pores that could provide a high specific surface to enabling cell attachment and bonding, and cell migration.

Patricio et al.(Patrício, Domingos et al. 2014) prepared two scaffolds based on the PCL and PLA blend by melting method and solvent casting via Biocell printing. The size of scaffolds pores was 311.6 ±17 µm (which was mixed by melting method) and 294±12 µm (which was mixed by solvent casting). A recent study reported 80 % porosity for a PLA/PCL/gelatin bone scaffold by freeze-drying method with an average pore size of 75 ± 3.2 µm which is lower than our PLA/PCL composite indicating the high porosity and pore size of the scaffold fabricated by thermal sintering method (Hashemi, Mehrabi et al. 2021).

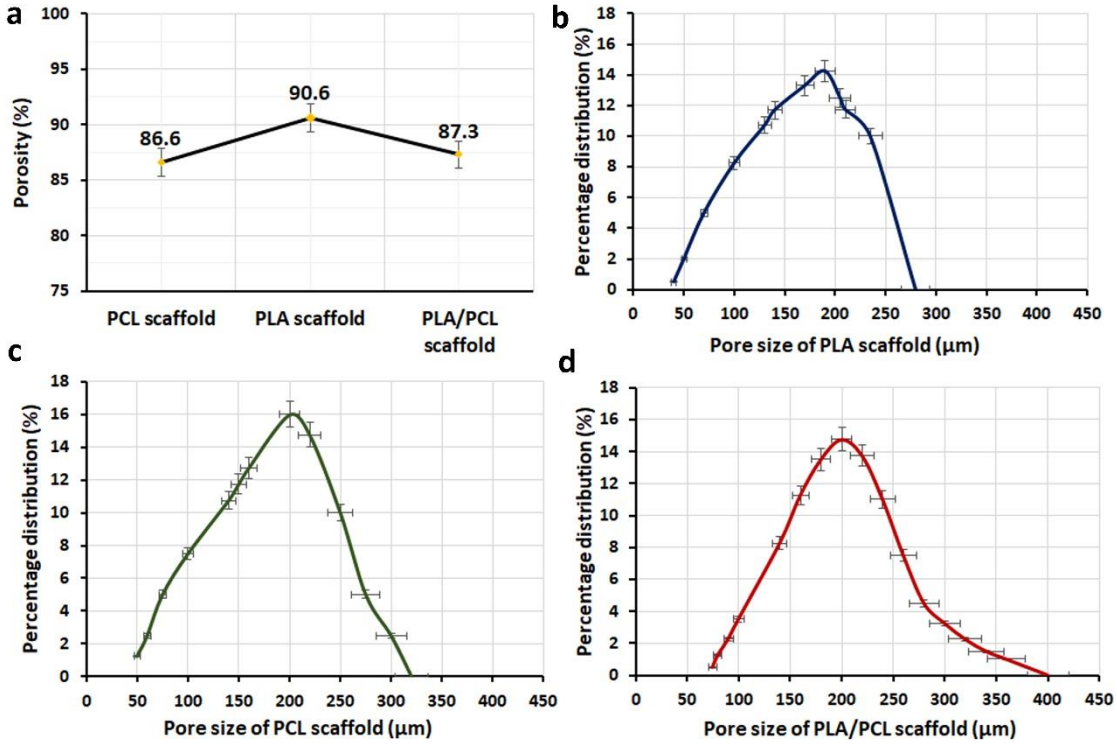

Fig. 3. (a) The percentage of porosity of the PCL, PLA, and PLA/PCL scaffolds, and the percentage of the distribution of pore size of (b) the PLA scaffolds, (c) the PCL scaffolds, and (d) the PLA/PCL composite scaffold.

Mechanical properties of PLA, PCL, and PLA/PCL scaffolds

Several characteristics of tissue engineering scaffolds such as substrate structure, composition, hydrophilicity, functional groups, and mechanical properties (particularly stiffness) significantly influence MSCs differentiation to encourage osteogenesis and influence proliferation(Yan, Sun et al. 2011, Mao, Shin et al. 2016). On the other hand, a scaffold should provide the required mechanical properties of the host tissue. Figure 4 shows the maximum of tensile stress (MPa) (a), Young's modulus (MPa) (b), and the maximum of tensile strain (mm/mm) (c) of the PLA, PCL, and PAL/PCL scaffolds. Generally, due to possessing more

aliphatic groups in its backbone, the PCL is more flexible than the PLA, which is evident in figure 4 (a-c). The PLA scaffold showed the highest maximum tensile stress, which was about 20.59 MPa, and this value for the PCL scaffold was 7.31 MPa, which was the lowest maximum tensile stress among the three scaffolds (figure 4 (a)). The maximum tensile stress of the PLA-PCL composite scaffold (14.66 MPa) was between the maximum tensile stress of the PLA and PCL scaffold (figure 4 (a)). A similar trend was observed for Young's modulus of the PLA, PCL, and PLA/PCL scaffolds that their Young's modulus was 63.23, 24.62, and 49.07 MPa, respectively (figure 4 (b)). By adding the PCL to the PLA, the maximum tensile strain of the PLA/PCL composite scaffold increased from 1.56 mm/mm, which was related to the PLA scaffold, to 7.67 mm/mm (figure 4 (c)). The PLA/PCL composite scaffold represents the mechanical properties between the PLA and PCL scaffold mechanical properties; therefore, the two polymers (PLA and PCL) had no improving effect on the mechanical properties of each other. Sankaran et al.(Sankaran, Krishnan et al. 2014) showed that by increasing the PLA content from 25 % to 75 % in the PLA/PCL blend nanofibers, the tensile strength increased from 1.0±0.3 MPa to 2.6±0.8 MPa, respectively. When the percentage of PCL in the scaffold decreased from 75 to 25 %, the tensile strain decreased from 7.4±2.3 % to 1.8±1.2 % either. This agrees with a previous study in which Jeong et al. showed that increasing the percentage of PLA in mixer improved the tensile strength. (Jeong, Rho et al. 2018).

Water uptake

Figure 4 (d) illustrates the water uptake of the PLA, PCL, and PLA/PCL scaffolds over time until 144 h. At the first 1 h, the scaffolds showed a rapid water uptake so that the water uptake values of the PLA, PCL, and PLA/PCL scaffolds were 9.8, 5.8, and 7.2 %, respectively. This initial rapid uptake can be due to the cavities and pores of the scaffolds that trapped the water. Hence, the PLA scaffold with high porosity (90.6 %) showed the highest water uptake. Torres et al.(Torres, Dominguez-Candela et al. 2020) showed that the water contact angle of the PCL decreased from 105° to 79.7° when it was blended with the PLA. The PLA is inclined to absorb water more than the PCL; hence, another possible reason it has a greater tendency to absorb water. The water uptake was slower from 1 to 12h, and it was 4.4, 4.9, and 4.5 % for the PLA, PCL, and PLA/PCL scaffolds, respectively. From 12 to 144h, the water uptake of the scaffolds reached the plateau, and the ultimate water up-takes was16.4 % for the PLA scaffold, 13 % for the PCL scaffold, and 14.2 % for the PLA/PCL scaffold. PCL scaffold showed the

lowest water uptake rate, which can be due to the hydrophobic nature of the PCL and the low porosity of the scaffold, which was 86.6 % (see figure 3 (a)).

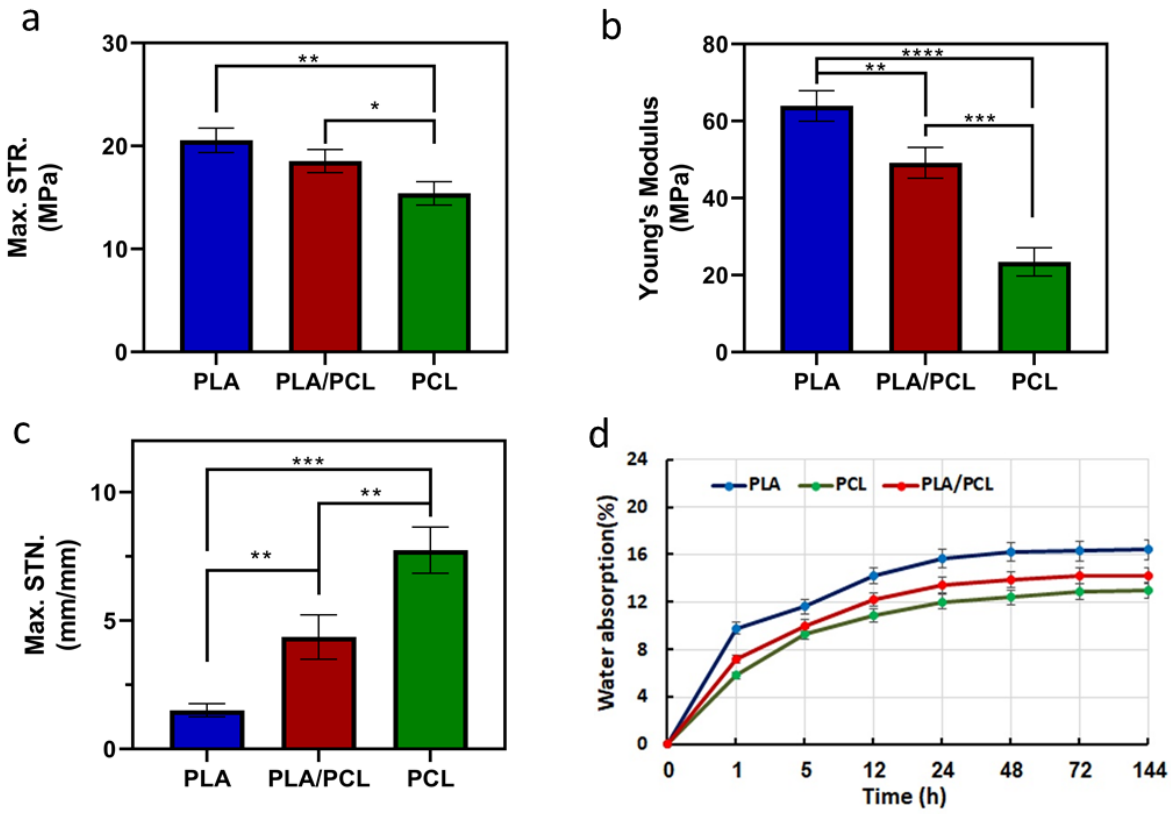

Fig. 4. Mechanical properties and water uptake of PCL, PCL and PCL/PLA scaffolds. (a) Maximum tensile stress (Max. STR.); (b) Young's modulus; (c) Maximum tensile strain (Max. STN.); (d) Water adsorption of Scaffolds. All experiments have been carried out in three replicates. Data were analyzed using a one-way ANOVA test. *$p < 0.05$; **$p < 0.005$, ***$p < 0.0005$, ****$p < 0.0001$

Accelerated degradation and biodegradation

The degradation process plays a vital role in designing and procurement of materials applicable to the biomedical field (Zhang, Zhou et al. 2014, Nie, Deng et al. 2020). The degradation process can be accelerated in two ways; first, by increasing the temperature of the degradation medium, and second by the addition of hydroxyl ions(Jafari, Shahrousvand et al. 2018). The degradation of sintered scaffolds (PLA, PCL, and PLA/PCL) over different periods of incubation in NaOH 1 M at 60 °C until 48 h (figure 5 (a)), and in SBF media at ambient temperature for 90 days (figure 5 (b)). The highest degradation is observed for the PLA scaffold after 90 days, which the remaining mass of PLA scaffolds at the end of 90 days was about 45

%. Water penetration into the scaffold structure improved PLA scaffold degradation. This could be due to PLA's hydrophilicity compared to the PCL and PLA/PCL scaffolds. Also, the high porosity of the PLA scaffold, which was 90.6 %, provided a more specific surface area for degradation. After 48 h of degradation in NaOH 1 M solution, the remaining mass was 21.6 %, 80.2 % and 53.33 % for the PLA, PCL and PLA/PCL scaffolds, respectively. Similar results were observed for biodegradation of the scaffolds in which the lowest degradation rate occurred for the PCL scaffold with 85 % remaining mass after 90 days.

Furthermore, the ultimate remaining mass of the PLA/PCL scaffold in the SBF was 70.5 %. The degradation rate of PLA-PCL scaffolds coated with gelatin nano-carriers made by freeze casting technique for 60 days in the SBF was studied by Shahrezaee et al. (Shahrezaee, Salehi et al. 2018). At the end of day 60, the weight loss of the scaffolds with a contact angle of 84.2° and 80.7° was about 40 %. Both polymers (PLA and PCL) degrade via cleavage of ester bonds of their backbone and change into acidic monomer that can accelerate the degradation process, and this acidic monomer can be disposed of by normal metabolic pathways from the body. The degradation rate of PLA and PCL is controlled by various factors such as molecular weight, crystallinity, temperature, absorbed water, and solubility of the degradation products (Sung, Meredith et al. 2004, Ghaffari-Bohlouli, Zahedi et al. 2020, Ghaffari-Bohlouli, Jafari et al. 2021).

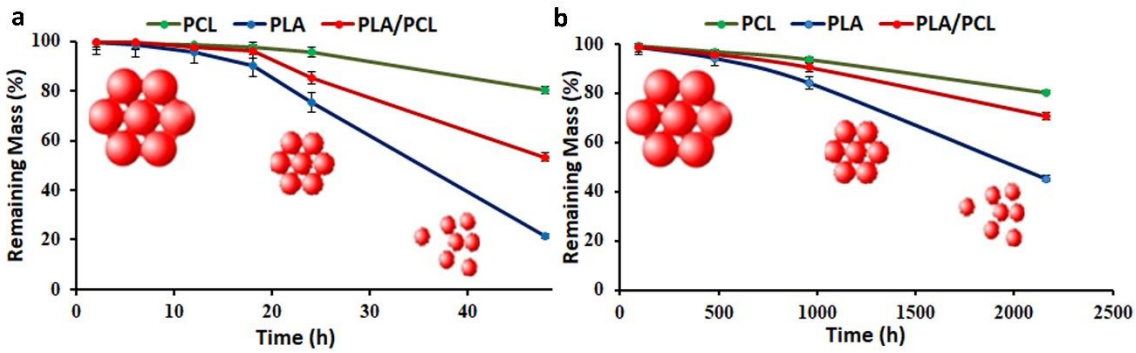

Fig. 5. The remaining mass of sintered scaffolds (PLA, PCL, and PLA/PCL) in accelerated medium (NaOH 1M) for 48h (a) and PBS for 90 days (b). The results are presented as mean ± SD.

Cytotoxicity

The biocompatibility of the PLA and PCL scaffolds prepared via different methods has been extensively shown in various studies (Ahmadzadeh, Babaei et al. 2018, Hernandez-

Martinez, Molina et al. 2018, Carvalho, Conde et al. 2020). The MTT assay was performed to evaluate the cell viability of sintered scaffolds (of the PLA, PCL, and PLA/PCL ones). Figure 6 illustrates the results of the MTT assay; during the assay time, the cell viability of all of the scaffolds had no remarkable difference with the control (TCPS) cell viability that shows the biocompatibility of the PLA, PLC, and PLA/PCL scaffolds. Although the cell viability of the sintered scaffolds at days 1, 4, and 7 did not cause a significant difference with the TCPS, the PLA, PCL, and PLA/PCL scaffolds showed a higher OD due to their porosity structure compared to the TCPS, so that the OD of the PLA/PCL sample at day 7 was 0.418 while for the TCPS was 0.405. The PLA sample had the highest OD between the other samples, which this value at days 1, 4, and 7 was 0.133, 0.335, and 0.425, respectively.

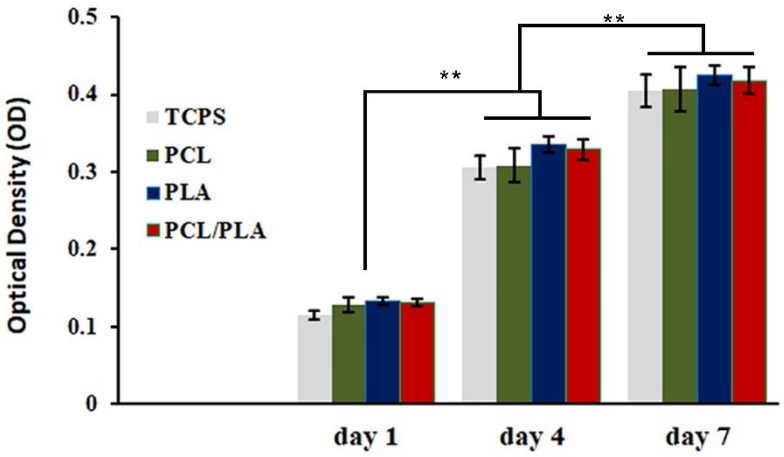

Fig. 6. MTT assay results show SNLs proliferation on sintered scaffolds after 1, 4 and 7 days of incubation. SNL76/7 cells were treated for 1, 3 and 5 days in the absence or presence of PCL, PLA, and PLA/PCL scaffolds. Results were expressed and were the mean ± SD of optical density of three independent experiments. Data were analyzed using a two-way ANOVA test.

Investigation of morphology and attachment characteristics of SNL 76/7 cells was used to examine the tendency of these cells to attach to the PLA, PCL, and PLA/PCL scaffolds when cells were cultured on those scaffolds. Figure 7 depicts the morphology of 1-cultured fibroblast cells on the PLA (a and b), the PCL (c and d), and the PLA/PCL scaffold (e and f) with two magnifications of 125X and 500X. The SNL 76/7 cells showed cell adhesion and spreading on the sintered scaffolds. From the MTT and cell attachment results, it can be concluded that the sintered PLA, PCL, and PLA/PCL scaffolds were not cytotoxic. The cell attachment results were supported by previous reports indicating the ability of PCL and PLA nanofibers for cells

adherence and growth of bone marrow stromal cells (BMSCs) and adipose-derived stem cells (ASCs) (Deng, Gu et al. 2015, Marei, El-Sherbiny et al. 2016).

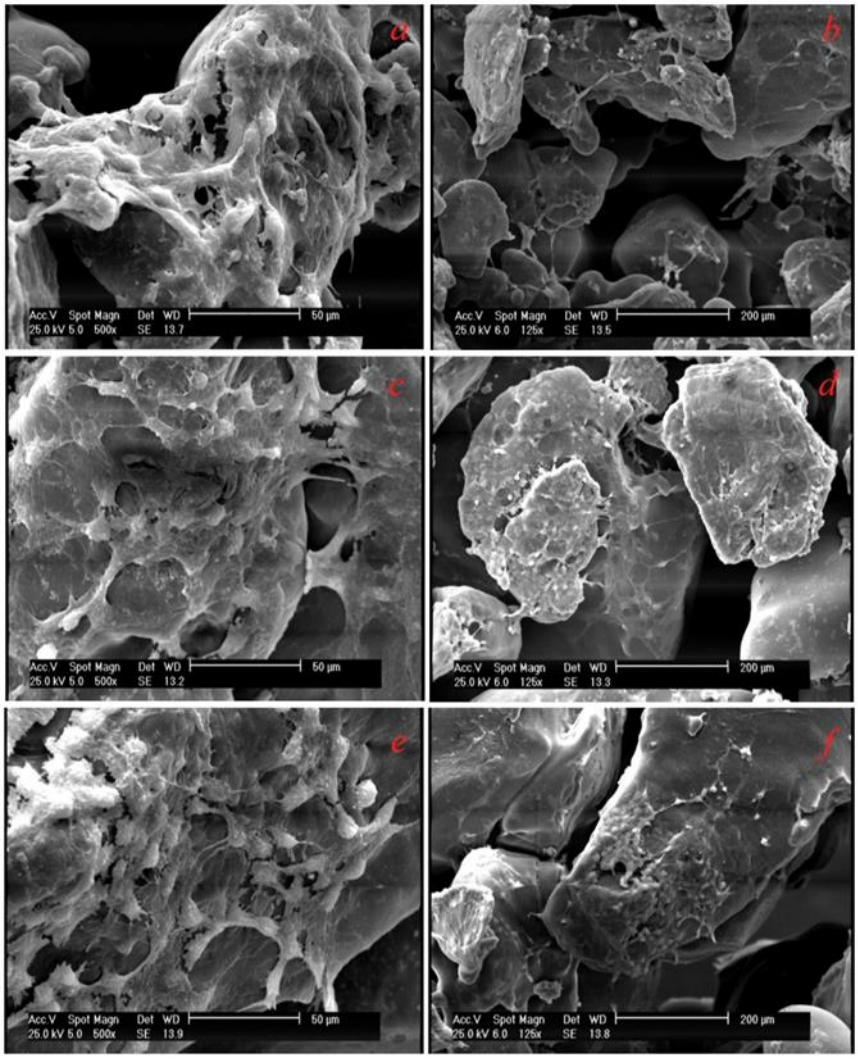

Fig. 4. SEM micrograph images of fibroblast cells (SNL76/7) attachment after 1 day of seeding on the PLA scaffold (a and b), the PCL scaffold (c and d), and the PLA/PCL scaffold (e and f).

Osteogenic markers assessment

The ALP activity is an early phenotypic marker expressed by osteoblast cells (Ghaffari-Bohlouli, Zahedi et al. 2020). The pattern of the ALP activity during osteogenic differentiation of MSCs on the sintered scaffolds was investigated on days 7 and 14 (figure 8 (a)). The ALP activity of hMSCs cells cultured on sintered scaffolds (the PLA, PCL, and PLA/PCL scaffolds) was remarkably higher (more than 2 times higher) than those cultured on control wells after 7 and 14 days. The PLA scaffold represented the highest ALP activity (0.64) compared to the PCL (0.61) and PLA/PCL (0.59) scaffolds after 14 days. After seeding the cells on a scaffold, MSCs begin to produce minerals indicating cell differentiation. The calcium content values in

figure 8 (b) show that the production of minerals increased for all the scaffolds. Like the ALP activity results, the PLA scaffolds had the highest calcium content (0,75 µg/scaffold) after 14 days compared to the other samples. The calcium content produced on the PLA, PCL, and PLA/PCL scaffolds at days 7 and 14 significantly differed compared to the TCPS sample. Yao et al. reported a significant improvement of ALP activity and calcium content of hMSCs cells treated by 3D electrospun PCL/PLA blend due to providing a favourable/desired microenvironment for cranial bone formation (Yao, Cosme et al. 2017).

The ALP activity and calcium content of all the sintered scaffolds were at the same level with no significant difference that can be concluded that the sintered method is an effective method to prepare bone scaffolds.

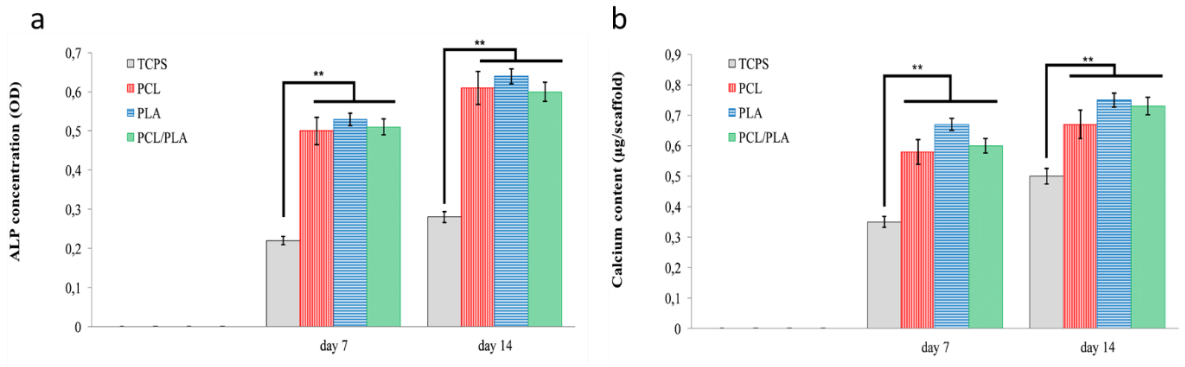

Fig. 8. The osteogenic mineralization analysis of the samples: (a) ALP analysis of hMSCs ($p < 0.05$) and (b) the measured OD levels of calcium minerals deposited by hMSCs due to osteogenic induction. Results were expressed as of ALP activity (OD) and calcium content (µg/scaffold) and were the mean ± SD of three independent experiments. Data were analyzed using a two-way ANOVA test. *$p < 0.05$; **$p < 0.005$ as compared to the control (TCSP).

Conclusions

The thermal sintering method was developed in the current study as a new approach to producing porous bone scaffolds using PLA, PCL, and their composite. Thermal Sintering of PLA and PCL composite (1:1) resulted in the 3D porous scaffold with a controlled pore size (75-400 µm) and high mechanical strength (elastic modulus of 191.39 MPa). Besides, the PCL scaffold's degradation rate and water uptake ability were improved upon mixing by PLA via the thermal sintering method. Additionally, the scaffolds were tested for their cytocompatibility and osteogenic differentiation ability, and the results confirmed that they failed to adversely affect the cell viability of fibroblasts (SNL 76/7). Furthermore, a significant increase in osteogenic differentiation of human Mesenchymal Stem Cells (hMSCs) has been demonstrated

using PCL, PLA, and their composite scaffolds assessed by ALP activity and calcium content measurement. Therefore, the thermal sintering method can be utilized as a promising fabrication method with a low cost and low complexity, particularly in the development of bone tissue scaffolds with high and controllable porosity.

Acknowledgments. HJ and AS acknowledge funding from Innoviris Brussels, Belgium (https://innoviris.brussels) under the project 2019 – BRIDGE – 4: RE4BRU. The content is solely the responsibility of the authors and does not necessarily represent the official views of the above-mentioned funding agency. The authors thank Mr. Mehdi Shahrousvand for his helpful comments.

Conflict of interest: The authors declare no conflict of interest.

References

Ahmadzadeh, Y., A. Babaei and A. Goudarzi (2018). "Assessment of localization and degradation of ZnO nano-particles in the PLA/PCL biocompatible blend through a comprehensive rheological characterization." Polymer Degradation and Stability **158**: 136-147.

Barral, V., S. Dropsit, A. Cayla, C. Campagne and É. Devaux (2021). "Study of the Influence of PCL on the In Vitro Degradation of Extruded PLA Monofilaments and Melt-Spun Filaments." Polymers **13**(2): 171.

Carvalho, J. R., G. Conde, M. L. Antonioli, P. P. Dias, R. O. Vasconcelos, S. R. Taboga, P. A. Canola, M. A. Chinelatto, G. T. Pereira and G. C. Ferraz (2020). "Biocompatibility and biodegradation of poly (lactic acid)(PLA) and an immiscible PLA/poly (ε-caprolactone)(PCL) blend compatibilized by poly (ε-caprolactone-b-tetrahydrofuran) implanted in horses." Polymer Journal **52**(6): 629-643.

Deng, M., Y. Gu, Z. Liu, Y. Qi, G. E. Ma and N. Kang (2015). "Endothelial differentiation of human adipose-derived stem cells on polyglycolic acid/polylactic acid mesh." Stem cells international **2015**.

Fang, R., E. Zhang, L. Xu and S. Wei (2010). "Electrospun PCL/PLA/HA based nanofibers as scaffold for osteoblast-like cells." Journal of nanoscience and nanotechnology **10**(11): 7747-7751.

Ghaffari-Bohlouli, P., H. Jafari, A. Khatibi, M. Bakhtiari, B. Tavana, P. Zahedi and A. Shavandi (2021). "Osteogenesis enhancement using poly (l-lactide-co-d, l-lactide)/poly (vinyl alcohol) nanofibrous scaffolds reinforced by phospho-calcified cellulose nanowhiskers." International Journal of Biological Macromolecules.

Ghaffari-Bohlouli, P., P. Zahedi and M. Shahrousvand (2020). "Enhanced osteogenesis using poly (l-lactide-co-d, l-lactide)/poly (acrylic acid) nanofibrous scaffolds in presence of dexamethasone-loaded molecularly imprinted polymer nanoparticles." International Journal of Biological Macromolecules **165**: 2363-2377.

Ghorbani, F., A. Zamanian, A. Shams, A. Shamoosi and A. Aidun (2019). "Fabrication and characterisation of super-paramagnetic responsive PLGA–gelatine–magnetite scaffolds with

the unidirectional porous structure: a physicochemical, mechanical, and in vitro evaluation." IET nanobiotechnology **13**(8): 860-867.
Hashemi, S. F., M. Mehrabi, A. Ehterami, A. M. Gharravi, F. S. Bitaraf and M. Salehi (2021). "In-vitro and in-vivo studies of PLA/PCL/gelatin composite scaffold containing ascorbic acid for bone regeneration." Journal of Drug Delivery Science and Technology **61**: 102077.
Hernandez-Martinez, A. R., G. A. Molina, R. Esparza, A. Luis Rodriguez, M. Cruz-Soto, E. Rodríguez-de León, D. Rangel and M. Estévez (2018). "Novel Biocompatible and Biodegradable PCL-PLA/Iron Oxide NPs Marker Clip Composite for Breast Cancer Biopsy." Polymers **10**(12): 1307.
Jafari, H., C. Delporte, K. Bernaerts, G. De Leener, M. Luhmer, L. Nei and A. Shavandi (2021). "Development of marine oligosaccharides for potential wound healing biomaterials engineering." Chemical Engineering Journal Advances: 100113.
Jafari, H., M. Shahrousvand and B. Kaffashi (2018). "Reinforced poly (ε-caprolactone) bimodal foams via phospho-calcified cellulose nanowhisker for osteogenic differentiation of human mesenchymal stem cells." ACS Biomaterials Science & Engineering **4**(7): 2484-2493.
Jafari, H., M. Shahrousvand and B. Kaffashi (2020). "Preparation and characterization of reinforced poly (ε-caprolactone) nanocomposites by cellulose nanowhiskers." Polymer Composites **41**(2): 624-632.
Jeong, H., J. Rho, J.-Y. Shin, D. Y. Lee, T. Hwang and K. J. Kim (2018). "Mechanical properties and cytotoxicity of PLA/PCL films." Biomedical engineering letters **8**(3): 267-272.
Koons, G. L., M. Diba and A. G. Mikos (2020). "Materials design for bone-tissue engineering." Nature Reviews Materials **5**(8): 584-603.
Lu, H. and S. G. Kazarian (2020). "How does high-pressure CO2 affect the morphology of PCL/PLA blends? Visualization of phase separation using in situ ATR-FTIR spectroscopic imaging." Spectrochimica Acta Part A: Molecular and Biomolecular Spectroscopy **243**: 118760.
Luciani, A., V. Coccoli, S. Orsi, L. Ambrosio and P. A. Netti (2008). "PCL microspheres based functional scaffolds by bottom-up approach with predefined microstructural properties and release profiles." Biomaterials **29**(36): 4800-4807.
Lv, Z., N. Zhao, Z. Wu, C. Zhu and Q. Li (2018). "Fabrication of novel open-cell foams of poly (ε-caprolactone)/poly (lactic acid) blends for tissue-engineering scaffolds." Industrial & Engineering Chemistry Research **57**(39): 12951-12958.
Mao, A. S., J.-W. Shin and D. J. Mooney (2016). "Effects of substrate stiffness and cell-cell contact on mesenchymal stem cell differentiation." Biomaterials **98**: 184-191.
Marei, N. H., I. M. El-Sherbiny, A. Lotfy, A. El-Badawy and N. El-Badri (2016). "Mesenchymal stem cells growth and proliferation enhancement using PLA vs PCL based nanofibrous scaffolds." International journal of biological macromolecules **93**: 9-19.
Mathieu, L., P.-E. Bourban and J.-A. Månson (2006). "Processing of homogeneous ceramic/polymer blends for bioresorbable composites." Composites Science and Technology **66**(11-12): 1606-1614.
Meskinfam, M., S. Bertoldi, N. Albanese, A. Cerri, M. C. Tanzi, R. Imani, N. Baheiraei, M. Farokhi and S. Fare (2018). "Polyurethane foam/nano hydroxyapatite composite as a suitable scaffold for bone tissue regeneration." Materials Science and Engineering: C **82**: 130-140.
Naghieh, S., M. K. Ravari, M. Badrossamay, E. Foroozmehr and M. Kadkhodaei (2016). "Numerical investigation of the mechanical properties of the additive manufactured bone scaffolds fabricated by FDM: the effect of layer penetration and post-heating." Journal of the mechanical behavior of biomedical materials **59**: 241-250.
Nahanmoghadam, A., M. Asemani, V. Goodarzi and S. Ebrahimi-Barough (2021). "Design and fabrication of bone tissue scaffolds based on PCL/PHBV containing hydroxyapatite

nanoparticles: dual-leaching technique." Journal of Biomedical Materials Research Part A **109**(6): 981-993.
Nail, L. N., D. Zhang, J. L. Reinhard and M. A. Grunlan (2015). "Fabrication of a bioactive, PCL-based" self-fitting" shape memory polymer scaffold." Journal of visualized experiments: JoVE(104).
Nie, L., Y. Deng, P. Li, R. Hou, A. Shavandi and S. Yang (2020). "Hydroxyethyl chitosan-reinforced polyvinyl alcohol/biphasic calcium phosphate hydrogels for bone regeneration." ACS omega **5**(19): 10948-10957.
Park, J. H., B. K. Lee, S. H. Park, M. G. Kim, J. W. Lee, H. Y. Lee, H. B. Lee, J. H. Kim and M. S. Kim (2017). "Preparation of biodegradable and elastic poly (ε-caprolactone-co-lactide) copolymers and evaluation as a localized and sustained drug delivery carrier." International journal of molecular sciences **18**(3): 671.
Patrício, T., M. Domingos, A. Gloria, U. D'Amora, J. Coelho and P. Bártolo (2014). "Fabrication and characterisation of PCL and PCL/PLA scaffolds for tissue engineering." Rapid Prototyping Journal.
Qu, H., H. Fu, Z. Han and Y. Sun (2019). "Biomaterials for bone tissue engineering scaffolds: a review." RSC advances **9**(45): 26252-26262.
Rao, R. U., B. Venkatanarayana and K. Suman (2019). "Enhancement of mechanical properties of PLA/PCL (80/20) blend by reinforcing with MMT nanoclay." Materials Today: Proceedings **18**: 85-97.
Sankaran, K. K., U. M. Krishnan and S. Sethuraman (2014). "Axially aligned 3D nanofibrous grafts of PLA–PCL for small diameter cardiovascular applications." Journal of Biomaterials Science, Polymer Edition **25**(16): 1791-1812.
Shahbazarab, Z., A. Teimouri, A. N. Chermahini and M. Azadi (2018). "Fabrication and characterization of nanobiocomposite scaffold of zein/chitosan/nanohydroxyapatite prepared by freeze-drying method for bone tissue engineering." International journal of biological macromolecules **108**: 1017-1027.
Shahrezaee, M., M. Salehi, S. Keshtkari, A. Oryan, A. Kamali and B. Shekarchi (2018). "In vitro and in vivo investigation of PLA/PCL scaffold coated with metformin-loaded gelatin nanocarriers in regeneration of critical-sized bone defects." Nanomedicine: Nanotechnology, Biology and Medicine **14**(7): 2061-2073.
Shahrousvand, M., F. A. Tabar, E. Shahrousvand, A. Babaei, M. M. Hasani-Sadrabadi, G. M. M. Sadeghi, H. Jafari and A. Salimi (2017). "High aspect ratio phospho-calcified rock candy-like cellulose nanowhiskers of wastepaper applicable in osteogenic differentiation of hMSCs." Carbohydrate polymers **175**: 293-302.
Shamsi, M., M. Karimi, M. Ghollasi, N. Nezafati, M. Shahrousvand, M. Kamali and A. Salimi (2017). "In vitro proliferation and differentiation of human bone marrow mesenchymal stem cells into osteoblasts on nanocomposite scaffolds based on bioactive glass (64SiO2-31CaO-5P2O5)-poly-l-lactic acid nanofibers fabricated by electrospinning method." Materials Science and Engineering: C **78**: 114-123.
Shavandi, A., A. E.-D. A. Bekhit, M. A. Ali and Z. Sun (2015). "Bio-mimetic composite scaffold from mussel shells, squid pen and crab chitosan for bone tissue engineering." International journal of biological macromolecules **80**: 445-454.
Shavandi, A., A. E.-D. A. Bekhit, Z. Sun and M. A. Ali (2016). "Bio-scaffolds produced from irradiated squid pen and crab chitosan with hydroxyapatite/β-tricalcium phosphate for bone-tissue engineering." International journal of biological macromolecules **93**: 1446-1456.
Shin, M., H. Abukawa, M. J. Troulis and J. P. Vacanti (2008). "Development of a biodegradable scaffold with interconnected pores by heat fusion and its application to bone tissue engineering." Journal of Biomedical Materials Research Part A: An Official Journal of The

Society for Biomaterials, The Japanese Society for Biomaterials, and The Australian Society for Biomaterials and the Korean Society for Biomaterials **84**(3): 702-709.
Sun, M. and S. Downes (2009). "Physicochemical characterisation of novel ultra-thin biodegradable scaffolds for peripheral nerve repair." Journal of Materials Science: Materials in Medicine **20**(5): 1181.
Sung, H.-J., C. Meredith, C. Johnson and Z. S. Galis (2004). "The effect of scaffold degradation rate on three-dimensional cell growth and angiogenesis." Biomaterials **25**(26): 5735-5742.
Torres, E., I. Dominguez-Candela, S. Castello-Palacios, A. Vallés-Lluch and V. Fombuena (2020). "Development and characterization of polyester and acrylate-based composites with hydroxyapatite and halloysite nanotubes for medical applications." Polymers **12**(8): 1703.
Vieira, A., J. Vieira, J. Ferra, F. Magalhães, R. Guedes and A. Marques (2011). "Mechanical study of PLA–PCL fibers during in vitro degradation." Journal of the mechanical behavior of biomedical materials **4**(3): 451-460.
Yan, C., J. Sun and J. Ding (2011). "Critical areas of cell adhesion on micropatterned surfaces." Biomaterials **32**(16): 3931-3938.
Yang, J., G. Shi, J. Bei, S. Wang, Y. Cao, Q. Shang, G. Yang and W. Wang (2002). "Fabrication and surface modification of macroporous poly (L-lactic acid) and poly (L-lactic-co-glycolic acid)(70/30) cell scaffolds for human skin fibroblast cell culture." Journal of Biomedical Materials Research: An Official Journal of The Society for Biomaterials, The Japanese Society for Biomaterials, and The Australian Society for Biomaterials and the Korean Society for Biomaterials **62**(3): 438-446.
Yao, Q., J. G. Cosme, T. Xu, J. M. Miszuk, P. H. Picciani, H. Fong and H. Sun (2017). "Three dimensional electrospun PCL/PLA blend nanofibrous scaffolds with significantly improved stem cells osteogenic differentiation and cranial bone formation." Biomaterials **115**: 115-127.
Zhang, H., L. Zhou and W. Zhang (2014). "Control of scaffold degradation in tissue engineering: a review." Tissue Engineering Part B: Reviews **20**(5): 492-502.